Gravitational radiation from realistic cosmic string loops

Paul Casper* and Bruce Allen†
Department of Physics, University of Wisconsin, Milwaukee, P.O. Box 413, Milwaukee, Wisconsin 53201
(Received 12 May 1995)

We examine the rates at which energy and momentum are radiated into gravitational waves by a large set of realistic cosmic string loops. The string loops are generated by numerically evolving parent loops with different initial conditions forward in time until they self-intersect, fragmenting into two child loops. The fragmentation of the child loops is followed recursively until only non-self-intersecting loops remain. The properties of the final non-self-intersecting loops are found to be independent of the initial conditions of the parent loops. We have calculated the radiated energy and momentum for a total of 11 625 stable child loops. We find that the majority of the final loops do not radiate significant amounts of spatial momentum. The velocity gained due to the rocket effect is typically small compared to the center-of-mass velocity of the fragmented loops. The distribution of gravitational radiation rates in the center of mass frame of the loops, $\gamma^0 \equiv (G\mu^2)^{-1}\Delta E/\Delta\tau$, is strongly peaked in the range $\gamma^0 = 45$–55; however, there are no loops found with $\gamma^0 < 40$. Because the radiated spatial momentum is small, the distribution of gravitational radiation rates appears roughly the same in any reference frame. We conjecture that in the center-of-mass frame there is a lower bound $\gamma^0_{\rm min} > 0$ for the radiation rate from cosmic string loops. In a second conjecture, we identify a candidate for the loop with the minimal radiation rate and suggest that $\gamma^0_{\rm min} \cong 39.003$.

PACS number(s): 98.80.Cq, 04.30.Db, 11.27.+d

I. INTRODUCTION

Cosmic strings are one-dimensional topological defects that may have formed if the vacuum underwent a phase transition at very early times [1–4]. The resulting network of strings is of cosmological interest if the strings have a large enough mass per unit length, μ. If $G\mu/c^2 \gtrsim 10^{-6}$, where G is Newton's constant and c is the speed of light (i.e., $\mu \gtrsim 10^{22}$ g/cm), then cosmic strings may be massive enough to have provided the density perturbations necessary to produce the large scale structure we observe in the Universe today.

The main constraints on μ come from observational bounds on the amount of gravitational background radiation emitted by cosmic string loops ([4–6] and references therein). A loop of cosmic string is formed when two sections of a long string (a string with length greater than the horizon length) meet and intercommute. Once formed, loops begin to oscillate under their own tension, undergoing a process of self-intersection (fragmentation) and eventually creating a family of non-self-intersecting oscillating loops. The gravitational radiation emitted by each loop as it oscillates contributes to the total background gravitational radiation. Determining the rate at which realistic loops radiate energy into gravitational waves is needed in constraining their mass per unit length, and thus understanding the potential cosmological importance of strings.

A number of calculations have been carried out to determine the rate at which special families of cosmic string loops convert their energy into gravitational radiation [7–10]. However, these loops all possess some amount of symmetry and therefore are not representative of realistic cosmic string loops. In order to generate a more realistic set of loops, Scherrer and Press used a fragmentation scheme where initial (parent) loops are evolved forward in time and are allowed to fragment into a set of (non-self-intersecting) child loops [11]. Because the properties of the child loops were found to be independent of the initial conditions used for the parent loops, they then argued that the child loops are representative of realistic cosmic string loops. Radiation rates for one such set of child loops were computed by Scherrer, Quashnock, Spergel, and Press (SQSP) [12] using a method developed by Quashnock and Spergel [13].

In a recent pair of papers, we introduced and tested a new method for calculating the rates at which energy and momentum are radiated by cosmic strings [14,15]. Using this new method, we investigated the special families of cosmic string loops previously examined in the literature. Our investigation found that many of the published radiation rates were numerically inaccurate (typically too low by a factor of 2). In order to apply our new method to more realistic sets of loops, as well as to provide an independent check of the work by SQSP, we have written a loop fragmentation code similar to that of Scherrer and Press which evolves initial (parent) loops forward in time until they self-intersect, fragmenting into two child loops. The fragmentation procedure is then performed recursively on the child loops until only non-self-intersecting loops remain. After successfully testing our fragmentation code on a large number (10 000) of loops for which

*Electronic address: pcasper@dirac.phys.uwm.edu
†Electronic address: ballen@dirac.phys.uwm.edu

the intersection points have been found analytically by Embacher [16], we used the code to fragment 900 parent loops, to generate a total of 12 418 child loops. Following Scherrer and Press [11], we used two sets of parent loops with very different initial conditions to generate the child loops. Several properties of the child loops (such as the size and velocity distributions) were compared to those of the loops generated by Scherrer and Press. As expected we find that both fragmentation codes have generated similar sets of child loops.

We also calculated the energy and spatial momentum radiated into gravitational waves for a total of 11 625 child loops. The distributions of the radiation rates of the child loops are found to be independent of the initial conditions used to generate the parent loops. We find that the majority of loops radiate their energy approximately spherically symmetrically, so that the radiated spatial momentum is small. We estimate that the velocity a loop gains due to the rocket effect is $v_r \lesssim 0.1c$. This is consistent with earlier numerical results [13] as well as heuristic estimates [17]. In the center of mass frame of a loop, the rate at which the loop loses energy to gravitational radiation is given by $\gamma^0 \equiv (G\mu^2)^{-1}\Delta E/\Delta\tau$, where here and throughout the rest of the paper τ is the proper time of the loop center of mass, G denotes Newton's constant, and we use units with the speed of light $c = 1$. The distribution of gravitational radiation rates is found to be strongly peaked in the range $\gamma^0 = 45$–55 and is similar to the distribution found by SQSP for loops with large γ^0. (SQSP calculate the gravitational radiation rates in the center-of-mass frame of the initial parent loops, but because the spatial momentum radiated is small, the distributions are similar in any reference frame.) However, our investigation has found a much sharper decrease in the number of loops with values of γ^0 smaller than 45, and unlike SQSP *we find absolutely no loops with* $\gamma^0 < 40$. We conjecture that in the center-of-mass frame, there are no realistic cosmic string loop configurations with γ^0 less than some $\gamma^0_{\rm min} > 0$. In a second conjecture, we identify a candidate for the cosmic string loop configuration with *the* smallest radiation rate, suggesting that $\gamma^0_{\rm min} \cong 39.003$.

The remainder of the paper is organized as follows. In Sec. II A, we describe the fragmentation code used to generate our set of realistic string loops. In Sec. II B, the analytic tests of our code are presented. Section II C compares the general properties of the loops generated by our fragmentation code with those generated by Scherrer and Press and establishes that the two fragmentation codes produce very similar sets of child loops. Section III starts with a review of how the radiation rates calculated in the center-of-mass frame of a loop are related to the rates viewed from any other reference frame. This is followed by an outline of the method used to calculate the rate at which energy and momentum are radiated into gravitational waves. The radiation rates are presented for the loops generated by our fragmentation code, and are compared to the results of SQSP. Two conjectures are made regarding the existence of a minimum energy radiation rate for any cosmic string loop. This is followed by a short conclusion.

II. GENERATION OF REALISTIC LOOP TRAJECTORIES

A cosmic string loop which is well inside the cosmological horizon is specified by the position $\mathbf{x}(t,\sigma)$ of the string as a function of two variables: time t and a spacelike parameter σ that runs from 0 to L. The total energy of the loop is μL where μ is the mass per unit length of the string, and L is referred to as the "invariant length" of the loop. If one examines only a single cycle of oscillation, and $G\mu << 1$, then gravitational back reaction may be neglected. In this case, the string loop satisfies equations of motion whose most general solution is

$$\mathbf{x}(t,\sigma) = \frac{1}{2}\left[\mathbf{a}(t+\sigma) + \mathbf{b}(t-\sigma)\right]. \quad (2.1)$$

Here, $\mathbf{a}$ and $\mathbf{b}$ are a pair of functions satisfying the "gauge condition" $|\mathbf{a}'(u)| = |\mathbf{b}'(v)| = 1$, where a prime denotes differentiation with respect to the function's argument. In the center-of-mass frame of the loop, $\mathbf{a}(u) \equiv \mathbf{a}(u+L)$ and $\mathbf{b}(v) \equiv \mathbf{b}(v+L)$. Because the functions $\mathbf{a}$ and $\mathbf{b}$ are periodic in this frame, each can be described by a closed curve in three-space. In this paper these curves are referred to as the $\mathbf{a}$ loop and the $\mathbf{b}$ loop. The gauge conditions ensure that the $\mathbf{a}$ and $\mathbf{b}$ loops are parametrized by their length. Together, the $\mathbf{a}$ and $\mathbf{b}$ loops define the trajectory of the string loop. In Sec. II A we outline the numerical code used to calculate the self-intersection points of an arbitrary string loop. Section II B provides the analytic tests of our code. In Sec. II C we describe the initial parent loops which were fragmented, and examine several of the properties of the resulting child loops. The energy and momentum radiated by the child loops are examined in Sec. III.

A. Fragmentation code

The functions $\mathbf{a}(t+\sigma)$ and $\mathbf{b}(t-\sigma)$ determine the shape of the string loop as a function of time. The condition for a loop to self-intersect at a time t_i is simply

$$\mathbf{x}(t_i,\sigma_1) = \mathbf{x}(t_i,\sigma_2) \quad (2.2)$$

or equivalently

$$\mathbf{a}(t_i+\sigma_1) + \mathbf{b}(t_i-\sigma_1) = \mathbf{a}(t_i+\sigma_2) + \mathbf{b}(t_i-\sigma_2), \quad (2.3)$$

with $\sigma_2 \neq \sigma_1 + nL$ for n an integer. In order to determine if a loop self-intersects, we divide the evolution of the loop over a single oscillation $(0 < t < L/2)$ into $6N$ time steps, where N is an integer typically in the range $N \in (200, 800)$. At each time step, N points are set down on the loop at regular intervals in σ. A piecewise linear approximation to the loop is then made by joining the N points with linear segments. Each segment is assumed to have a constant velocity, given by the velocity of the string loop at the point halfway between the ends of the linear segment. The $O(N^2)$ pairs of segments are then compared to see if any will cross within the next time step. This introduces a lower bound of $O(L/N)$ on the size of the smallest child loop which can be found by our code.

A crossing is detected by first finding the time t_0 at which the volume of the tetrahedron defined by the four end points of the two segments goes to zero. This is easy to compute since the segments are assumed to have constant velocity. If the time t_0 is within the next time step, then it is possible that an intersection may occur during that time step. The vanishing tetrahedron volume only means that the lines defined by the two segments are coplanar; it does not ensure that the intersection point lies on both (or either) of the two linear segments. We calculate the intersection point of the two lines to check whether the two segments actually cross. If they do, then a possible intersection has been located. The intersection is characterized by the three coordinates $(t_0, \sigma_1, \sigma_2)$, where σ_1 and σ_2 are the spatial coordinates of the intersection point on the two linear segments. However, since the piecewise linear loop is only an approximation, the intersection found above may not correspond to a true intersection on the real loop. Furthermore, even if a true intersection does occur, the values $(t_0, \sigma_1, \sigma_2)$ would only locate it approximately. In order to find the exact intersection point, Eq. (2.3) is solved using the Newton-Raphson method with $(t_0, \sigma_1, \sigma_2)$ supplied as the initial trial solution, using the exact expressions (not the piecewise linear approximation) for the loop's trajectory. Given a sufficiently good trial solution, the Newton-Raphson method will always converge to the exact intersection point if one exists. Each pair of linear segments is checked for an intersection. It is possible that more than one intersection will be found in a given time step. In this case, the fragmentation takes place at the earliest intersection.

The method we use to detect intersections is slightly different from that used by Scherrer and Press. In their code, linear segments are used to approximate the **a** and **b** loops. This gives rise to a piecewise linear loop with approximately the same shape as the real loop. The volumes of the tetrahedrons formed by the different pairs of segments on the approximate loop are then used to determine potential crossings as above. The difference is that with our method, the kinks joining the linear segments are always equally spaced (in σ) while the spacing between any two kinks in the Scherrer-Press method is a function of time.

When a string loop self-intersects, it fragments into a pair of child loops. The **a** and **b** loops which define the trajectories of the two child string loops are simply related to the **a** and **b** loops of the parent string loop [11]. At the instant the fragmentation takes place, the two intersecting points on the parent string loop correspond to two points on both its **a** loop and its **b** loop. The **a** and **b** loops for the two child loops are generated by breaking the parent **a** and **b** loops at these points, and then continuing each piece of the curve periodically in three-space. The child **a** and **b** loops generated in this way will not be closed curves. This is because the center of mass of each child string loop will be in motion relative to the center-of-mass frame of the parent string loop. After the parent loop has fragmented, each child loop is then fragmented recursively until only non-self-intersecting loops remain. The **a** and **b** loops of each child string loop are known analytically since they are composed of sections of the known **a** and **b** loops of the original parent string loop. Thus, the trajectory of each child loop may be determined with the same accuracy as that of the initial parent loop.

B. Testing the fragmentation code

The self-intersection points for Turok's two-parameter family of cosmic string loops [18] have been determined analytically by Embacher [16]. The **a** and **b** loops which define this family of string loops are given by

$$\begin{aligned} \mathbf{a}(u) &= \sin(u)\hat{\mathbf{x}} - [\cos(\phi)\hat{\mathbf{y}} + \sin(\phi)\hat{\mathbf{z}}]\cos(u), \\ \mathbf{b}(v) &= [(\alpha-1)\sin(v) - \tfrac{1}{3}\alpha\sin(3v)]\hat{\mathbf{x}} + [(\alpha-1)\cos(v) - \tfrac{1}{3}\alpha\cos(3v)]\hat{\mathbf{y}} - 2\sqrt{\alpha(1-\alpha)}\cos(v)\hat{\mathbf{z}}. \end{aligned} \tag{2.4}$$

The parameters α and ϕ are constrained to satisfy $0 \le \alpha \le 1$ and $-\pi \le \phi \le \pi$. However, the symmetries in this family of loops allow one to restrict attention to $0 \le \phi \le \pi/2$.

To test our code, we have fragmented 10 000 loops from this family, and compared them to Embacher's analytic results. Embacher has calculated the fragmentation points for the initial Turok loops only. The loops are not allowed to intercommute. Thus, for this test, we allowed our code to run only until the first fragmentation occurs (or through one full oscillation if the loop does not self-intersect). The number of linear segments used at each time step to locate the approximate loop crossings was $N = 200$ for each of the test loops. The two-dimensional parameter space was divided into a (100×100) grid of loops with $0 < \alpha < 1$ and $0 < \cos(\phi) < 1$. Figure 1 shows the results of our numerical fragmentation code. Loops which were found to self-intersect are shown as dark dots. Loops for which no intersection was found are shown as light dots. Also shown is the analytic boundary derived by Embacher dividing the parameter space into self-intersecting and non-self-intersecting loops. Our fragmentation code is in perfect agreement with the analytic predictions. In the cases where an intersection was predicted, the coordinates characterizing the intersection, $(t_i, \sigma_1, \sigma_2)$, found by our code typically agreed to six decimal places with the predicted values. This agreement gives us good confidence that our fragmentation code calculates intersection points correctly.

C. Fragmentation results

A realistic set of string loop trajectories may be generated by loop fragmentation in the following way. Parent

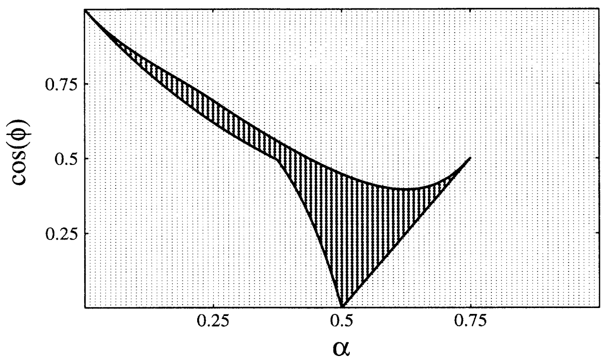

FIG. 1. The figure shows 10 000 loops from Turok's two-parameter family of cosmic string loops defined by the parameters α and ϕ. Loops which our code found to be self-intersecting are shown as dark dots. Loops for which our code found no self-intersection are shown as light dots. The closed solid curve shows Embacher's analytic result dividing the parameter space into regions corresponding to self-intersecting and non-self-intersecting loops. It is in perfect agreement with our fragmentation code.

loops with very different initial conditions are recursively fragmented into non-self-intersecting child loops. If the properties of the final child loops are similar, independent of the initial conditions used for their parent loops, then they should be representative of the properties of realistic cosmic string loops. We follow Scherrer and Press [11] in the choice of what parent loops to fragment, and begin with two sets of loops having very different initial conditions. We take the **a** and **b** loops defining all the parent loops to be of the form

$$\mathbf{a}_x(s) = \sum_{m=1}^{M} a_{xm} \cos(ms + \phi_{xm}), \tag{2.5}$$

with similar equations for $\mathbf{a}_y, \mathbf{a}_z$, and **b**. It should be noted that s is not the length along the **a** loop. The actual length $u(s)$ must be computed numerically. Following Scherrer and Press, we take $M = 10$ and take the ϕ's to be random numbers in the range $[0, 2\pi]$. For the first set of parent loops (referred to as type A loops), the $\mathbf{a}_m$ and $\mathbf{b}_m$ coefficients are chosen to be random numbers between 0 and 1. This gives equal amplitude to both the high and low frequency modes, resulting in highly convoluted initial loops which each fragment into a large number of child loops. For the second set of parent loops (referred to as type B loops), the $\mathbf{a}_m$ and $\mathbf{b}_m$ coefficients are chosen to be random numbers between 0 and $1/m^2$. This gives smaller amplitude to the high frequency modes and results in loops which are much less convoluted than the type A loops. As one would expect, the type B loops typically fragment into a much smaller number of child loops.

We have fragmented a total of 900 parent loops (200 type A, 700 type B). This resulted in a total of 12 418 child loops (5723 from type A parents, 6695 from type B). At each time step when fragmenting loops of type B, a total of $N = 400$ linear segments were used to find the approximate intersection points. For the more convoluted type A loops, this number was increased to $N = 600$. For both the type A and B cases, a number of loops were rerun with N increased by 200. In both cases this resulted in almost no new child loops being formed. Thus, we are confident that we are not missing a large number of small loops just below the resolution of our code.

We compared the loops generated by our fragmentation code to those generated by Scherrer and Press [11]. Scherrer and Press fragmented a total of 100 parent loops (20 type A, 80 type B) for a total of 1 172 child loops (561 from type A parents, 611 from type B). The two codes produce very similar sets of child loops. The only differences are due to the better statistics of our results and the slightly higher resolution of our code. (Scherrer and Press use 256 linear segments to approximate both types of loops in their simulations.) Details of the comparisons between the different sets of child loops are given below.

Our fragmentation code evolves each parent loop forward in time, checking for fragmentations. If the loop does self-intersect, then the fragmentation procedure is carried out recursively on each of the child loops until only non-self-intersecting loops remain. The mean number and standard deviation of stable child loops generated by our code per parent loop are 29 ± 6 (type A) and 10 ± 4 (type B). This is slightly higher than the values 28 ± 6 (type A) and 8 ± 4 (type B) found by Scherrer and Press. The slightly larger mean values found by our investigation are due partly to improved statistics and partly to the higher resolution of our code. The larger number of segments used by our code to approximate the loop at each time step allows us to detect smaller loop fragmentations than was previously possible.

The number of stable child loops of a given generation are shown in Fig. 2. (The initial parent loops are first generation, their direct children are second generation, etc.) The results for child loops descended from loops of type A and B are shown in Figs. 2(a) and 2(b), respectively. For comparison, the equivalent results found by Scherrer and Press are shown in Figs. 2(c) and 2(d). It should be noted that because the total number of loops represented in each of the graphs is different, the scales on the vertical axes are also different. The scales have been chosen to allow direct comparison between the different graphs. As expected, the more convoluted type A loops undergo more fragmentation than the B loops and typically result in stable child loops of a higher generation. The larger mean number of child loops found by our code causes the peaks of the distributions in Figs. 2(a) and 2(b) to lie slightly to the right of the respective peaks in Figs. 2(c) and 2(d). In addition, because we examine more than 10 times the number of stable child loops than Scherrer and Press, we find much less statistical noise in our results. However, the overall distributions have very similar shapes.

The invariant length distributions of the stable child loops are shown in Fig. 3. Figures 3(a) and 3(b) show the results for child loops descended from type A and type B loops, respectively. The equivalent results found by Scherrer and Press are shown in Figs. 3(c) and 3(d). All

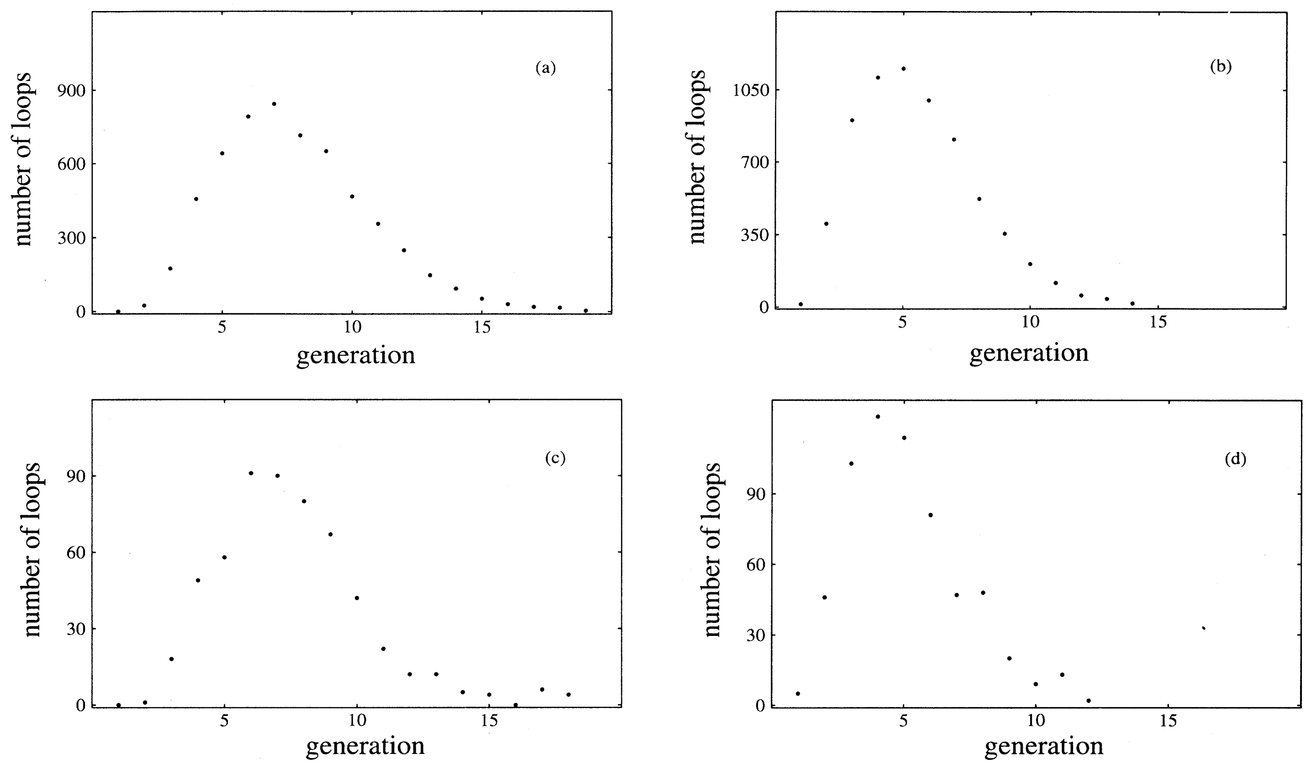

FIG. 2. The number of stable child loops belonging to a given generation and having initial parent loops of (a) type A and (b) type B. The corresponding results found by Scherrer and Press are given in (c) and (d).

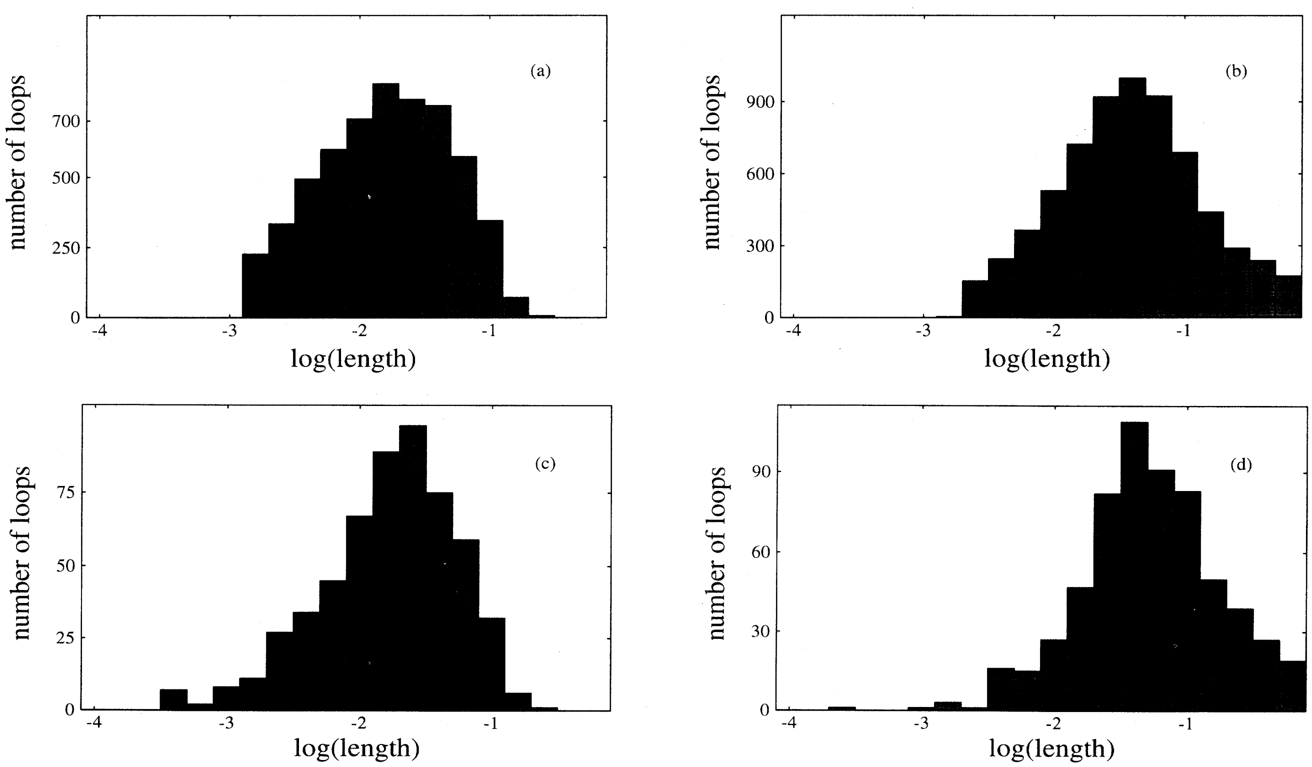

FIG. 3. The number of stable child loops with a given invariant length having initial parent loops of (a) type A and (b) type B. The corresponding results found by Scherrer and Press are given in (c) and (d). All the lengths are given in units where the initial parent loop length is 1. The logarithms are base 10.

of the lengths are given as a fraction of the initial parent loop's length, which we set equal to 1. Because the A loops undergo more fragmentation, the size distribution in this case is centered around smaller lengths than in the B case.

Comparing our results to those found by Scherrer and Press, we find that overall the distributions look similar. However, there are two differences worth noting. First, while the peaks of the distributions are at roughly the same place, a slightly larger fraction of loops are found to the left of the peaks in our results. This increase in the number of loops of relatively small size is again due partly to better statistics and partly to the increased resolution of our code. The second difference has to do with loops of extremely small size. We impose an artificial cutoff of order $(1/N)$ on the minimum loop size generated by our code. This cutoff is equal to the size of the smallest loop that could be fragmented off of one of the initial parent loops. Even though the same number of segments are used to detect fragmentations on each child loop, this cutoff is still imposed. Thus, our distributions have no loops with length less than $\sim (1/600)$ in Fig. 3(a) and $\sim (1/400)$ in Fig. 3(b). While Scherrer and Press have a cutoff of $\sim (1/256)$ for the size of the smallest loop fragmented off their parent loops, they do not impose this cutoff on the subsequent child loops. If a child loop has length 0.1, then that loop is allowed to generate a child of its own with length as small as $\sim (0.1/256)$. Thus their code allows very small loops to be formed through multiple fragmentations. However, these very small loops are biased in that they can only come from loops that are already small. Figures 3(c) and 3(d) show that there are very few loops generated in this way which have length smaller than the cutoff we impose.

The total momentum of the string loops is conserved when fragmentation takes place. Thus, when small loops are fragmented off of larger ones, they typically have large center-of-mass velocities. To determine whether the loops used in this investigation break roughly in half, or whether they tend to break off small child loops, one can define a fragmentation fraction f to each fragmentation which occurs. This fraction is given by the ratio of the length of the smaller of the two child loops to the length of the parent loop $(0 < f \leq 0.5)$. Figures 4(a) and 4(b) show the number of fragmentations with a given value of f for the type A and B loops, respectively. Figures 4(c) and 4(d) show the equivalent results found by Scherrer and Press. While there is a larger amount of statistical noise in Figs. 4(c) and 4(d), these distributions are seen to be fairly similar to those in Figs. 4(a) and 4(b). The tendency of the type B loops to form child loops of unequal size (small f) is clearly shown in Figs. 4(b) and 4(d). This tendency is also found to a lesser extent for the type A loops as is shown in Fig. 4(a). In all four cases, the decrease in the smallest f bin is due to the artificial cutoff introduced by the procedure used for finding the fragmentations. The larger number of fragmentations found in the lowest f bins in Figs. 4(a) and

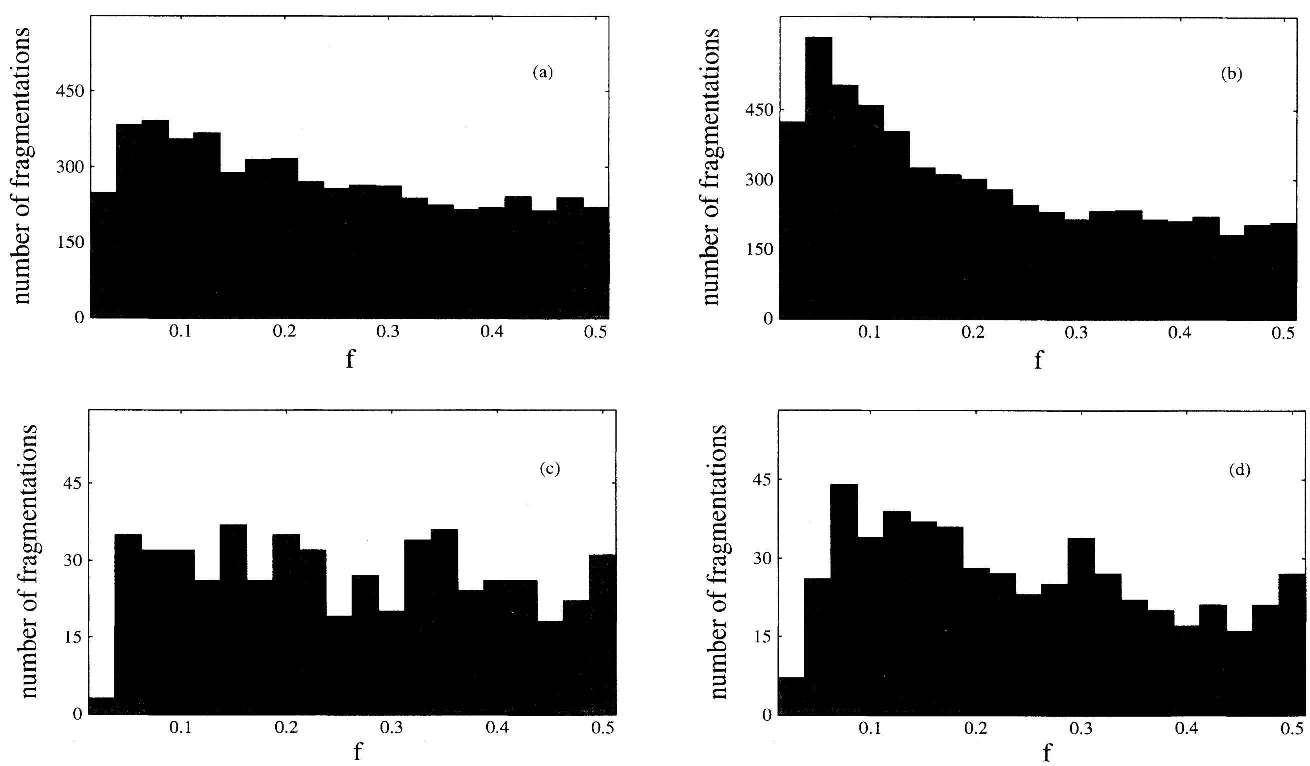

FIG. 4. The number of fragmentations with a given fragmentation fraction f for loops having initial parent loops of (a) type A and (b) type B. Here f is the ratio of the length of the smaller of the two child loops to the length of the immediate parent loop. The corresponding results found by Scherrer and Press are given in (c) and (d).

4(b) are a result of the high resolution of our code.

The tendency of fragmentations to form child loops of unequal size has a dramatic effect on the velocity distribution of the loops. When a small loop is fragmented off of a much larger loop, it is typically formed with a large center-of-mass velocity. Figures 5(a) and 5(b) show the velocity distributions of the stable child loops descended from type A and type B parents respectively. The mean velocity and standard deviation are $v/c = 0.60 \pm 0.26$ for case A and $v/c = 0.73 \pm 0.26$ for case B. The equivalent velocity distributions found by Scherrer and Press are shown in Figs. 5(c) and 5(d), and have mean velocities and standard deviations of $v/c = 0.55 \pm 0.24$ and $v/c = 0.64 \pm 0.25$ respectively. All of the velocities are specified with respect to the center-of-mass frame of the initial parent loops.

In this section we have shown that the stable child loops generated by our fragmentation code are very similar to those generated by Scherrer and Press, and argued that the small differences are due to the improved statistics of our results and the better resolution of our code.

III. GRAVITATIONAL RADIATION

As cosmic string loops oscillate, they lose their energy in the form of gravitational radiation. If a loop radiates its energy in a non-spherically-symmetric pattern, then the loop will also radiate spatial momentum. In this section we examine the rates at which the stable child loops described in Sec. II radiate energy and spatial momentum.

The rates at which a cosmic string loop radiates energy and spatial momentum as observed in the center-of-mass frame are easily related to the rates observed in any other frame. If we define the four-momentum of the gravity waves emitted by a string loop in its center-of-mass frame to be $P^\alpha = (E, \mathbf{P}) = (E, P^i)$, where $i = x, y, z$, then the average rate of energy and momentum loss by an oscillating string loop in that frame is given by $\Delta P^\alpha / \Delta\tau$, where

$$\frac{\Delta P^\alpha}{\Delta\tau} = \left(\frac{\Delta E}{\Delta\tau}, \frac{\Delta \mathbf{P}}{\Delta\tau}\right) = G\mu^2(\gamma^0, \gamma^i). \qquad (3.1)$$

Here, $\Delta E/\Delta\tau$ is the energy radiation rate (i.e., the power) and $\Delta P^i/\Delta\tau$ are the three spatial components of the momentum radiation rate. All four quantities are averaged over a single oscillation of the loop. In any given reference frame, the dimensionless quantities $\gamma^\alpha = (\gamma^0, \gamma^i)$ depend only upon the shape of the cosmic string loop as it oscillates. They are invariant under a rescaling (magnification or shrinking) of the loop, provided that the velocity at each point on the rescaled loop is unchanged.

Because γ^α is a four-vector, we may easily calculate its components in any other frame of reference. For example, in a frame which is moving at velocity $\mathbf{w}$ in the center-of-mass frame,

$$\tilde{\gamma}^0 = \Gamma(\gamma^0 - w_i \gamma^i) \qquad (3.2)$$

and

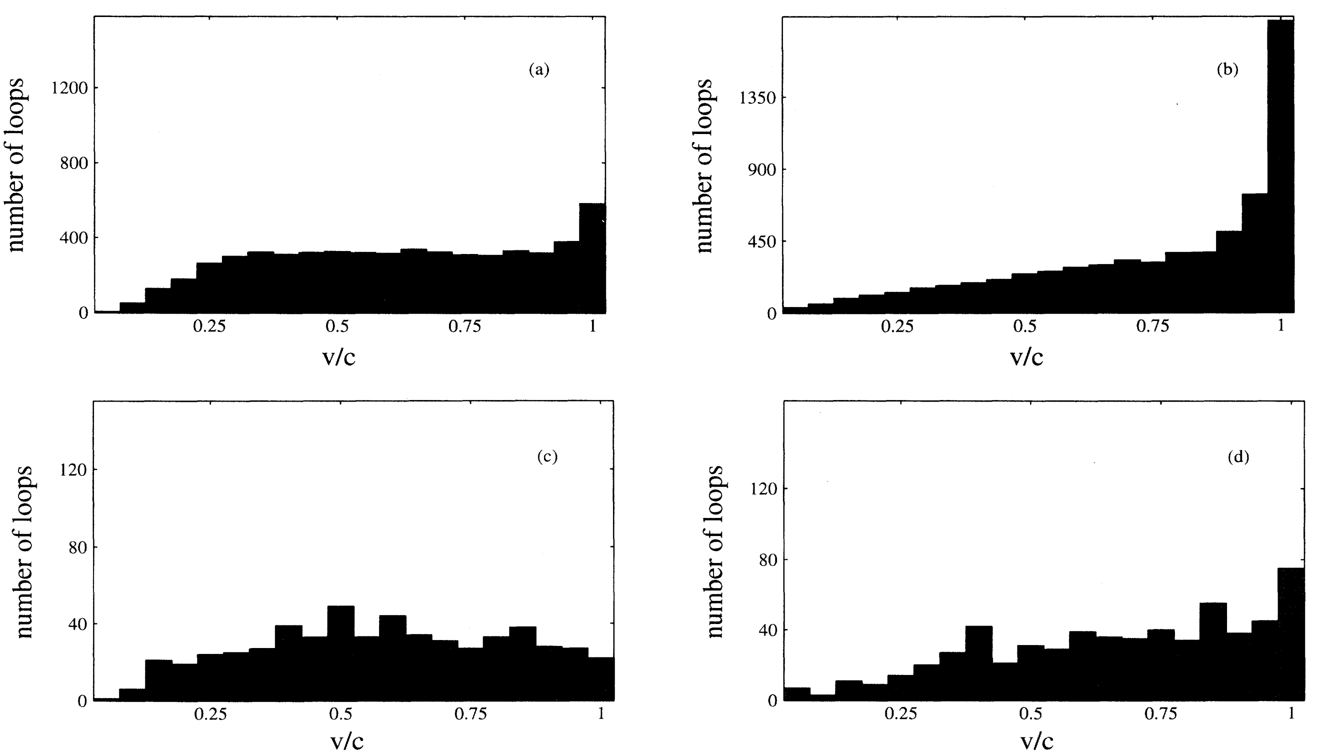

FIG. 5. The number of stable child loops with a given center-of-mass speed $v = |\vec{v}|$ with initial parent loops of (a) type A and (b) type B. The corresponding results found by Scherrer and Press are given in (c) and (d). The speed of each child loop is measured in the center-of-mass frame of the initial parent loop.

$$\tilde{\gamma}^i = \gamma^i + \frac{(\Gamma - 1)}{w^2}(w_j\gamma^j)w^i - \Gamma\gamma^0 w^i, \quad (3.3)$$

where $w \equiv |\mathbf{w}|$ and $\Gamma \equiv (1 - w^2)^{-1/2}$. These equations are simply the transformation laws of four-vectors (Eqs. 11.19 of [19]). *Note, however, that the observed radiation rates in this new frame differ from $\Delta\tilde{P}^\alpha/\Delta\tau = G\mu^2\tilde{\gamma}^\alpha$ by a factor of $1/\Gamma = \Delta\tau/\Delta t$.* The correct radiation rates as observed in the new frame are

$$\frac{\Delta\tilde{P}^0}{\Delta\tilde{t}} = \frac{1}{\Gamma}\frac{\Delta\tilde{P}^0}{\Delta\tau} = \frac{G\mu^2}{\Gamma}\tilde{\gamma}^0 = G\mu^2(\gamma^0 - w_i\gamma^i) \quad (3.4)$$

and

$$\frac{\Delta\tilde{P}^i}{\Delta\tilde{t}} = \frac{1}{\Gamma}\frac{\Delta\tilde{P}^i}{\Delta\tau} = \frac{G\mu^2}{\Gamma}\tilde{\gamma}^i = G\mu^2\left(\frac{\gamma^i}{\Gamma} + \left(1 - \frac{1}{\Gamma}\right)w^{-2}(w_j\gamma^j)w^i - \gamma^0 w^i\right). \quad (3.5)$$

Thus the numerical values found for the radiation rates depend upon the observer's frame of reference. In the work of SQSP [12] it is stated that "Our γ values have been calculated in the parent loop center of mass, in which the daughter loops can have large velocities, but the results would be the same if calculated in the rest frame of the daughter loops"; this statement is not true unless $\gamma^i = 0$ in which case no spatial momentum is radiated in the center-of-mass frame. We note, however, that because the radiated spatial momentum in the center-of-mass frame is typically small (as shown below) the gravitational radiation rate observed in any frame will differ by only a few percent from that observed in the center-of-mass frame [20].

To calculate the radiation rates of the child loops generated by our fragmentation code, we have used the piecewise linear method developed by Allen, Casper, and Ottewill [14,15]. This method calculates γ^α exactly in the center-of-mass frame for any loop for which the **a** and **b** loops are composed of piecewise linear segments. Accurate radiation rates for smooth loops are found by approximating the smooth **a** and **b** loops with piecewise linear ones. This method has been carefully tested, both against other methods and against a large class of loops for which the exact radiation results are known [10,14,15].

We have calculated the γ^α values for a total of 11 625 non-self-intersecting child loops (5305 descended from type A parents, 6320 from type B). Each loop was boosted into its center-of-mass frame, and the (now closed) **a** and **b** loops were approximated with 48 segments each. When testing the piecewise linear method, it was found that the percent error in γ^α was approximately given by $200/N$, where N is the total number of segments used to approximate the string loop. Since we have used a total of $N = 96$ segments for each loop, we expect errors of no more than a few percent.

The distributions of gravitational radiation rates for the stable child loops are shown in Figs. 6 and 7. Figures 6(a) and 6(b) show the results for loops descended from type A and B parents respectively. Figures 7(a) and 7(b) show the same results, but with 10 times the number of γ^0 bins. The distributions have very similar shapes, independent of the initial parent loop type. We have also calculated the radiation rates in three other reference frames: the parent loop center-of-mass frame, the frame in which the net spatial momentum radiated is zero ($w^i = \gamma^i/\gamma^0$), and the frame in which the energy radiation rate appears smallest [$w^i = \gamma^i/(\gamma_j\gamma^j)$]. Because the radiated spatial momentum is typically small (as shown below), the individual radiation rates are not greatly changed, and the distributions appear very similar in all four frames. In particular, the distributions all show the dramatic fall off in the number of loops with $\gamma^0 < 45$.

For comparison, the distributions of gravitational radiation rates found by SQSP [12] are shown in Figs. 6(c) and 6(d). SQSP calculated energy radiation rates in the parent loop center-of-mass frame for 455 child loops (240 descended from type A parents, 215 from type B). Both their results and our own find the distribution of loops to be peaked near $\gamma^0 = 50$, and to fall off rapidly for larger values. There is, however, a dramatic difference in the results for $\gamma^0 \lesssim 40$. While SQSP find a small number of loops with very low values of γ^0, we find that the distributions fall off extremely rapidly for $\gamma^0 < 44$, and *did not find a single loop with $\gamma^0 < 40$.* (It has been suggested [20] that for certain loops, a lack of numerical resolution in the computer code used to calculate γ^0 could explain the lowest γ^0 values reported in [12].) Although the dramatic cutoff in the distribution of gravitational radiation rates is a new result, a nonzero lower bound on γ^0 was not totally unexpected.

There are several reasons why a nonzero lower bound on γ^0 was not surprising. One reason is that an investigation of all loop trajectories previously studied by other authors found that none of those trajectories had $\gamma^0 < 44$ [14], where here and below we consider only radiation rates in the center-of-mass frame. A second piece of evidence comes from a specific class of cosmic string loop trajectories which we have recently studied, for which exact γ^0 values are known [10]. String loops within this specific class are defined by **a** and **b** loops which have the following form. The **a** loop is a closed curve consisting of two equal length, colinear, straight segments. The **b** loop is constrained to lie in the plane perpendicular to the **a** loop. The loop trajectory with the absolute minimum value of γ^0 for any loop in this specific class has been identified and has

$$\gamma^0 = 16\int_0^{2\pi} dx\, \frac{1 - \cos(x)}{x} \cong 39.003. \quad (3.6)$$

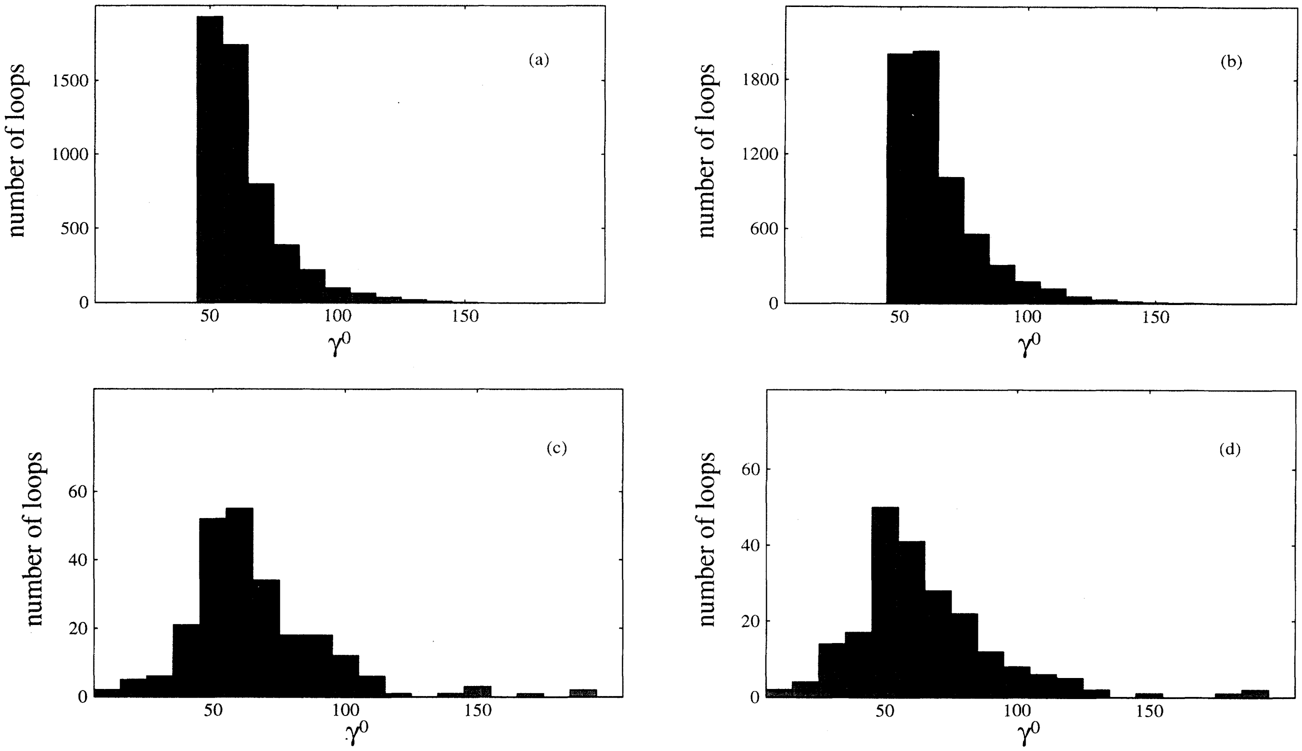

FIG. 6. The number of stable child loops with a given rate of energy loss in gravitational radiation, in units of $G\mu^2$, for initial parent loops of (a) type A and (b) type B. Each bin has width 10. The corresponding results found by SQSP are given in (c) and (d).

The **b** loop in this case has the shape of a perfect circle (traversed once) as shown in Fig. 8(a). This string loop has the lowest value of γ^0 which is currently known.

Finally, given the mounting evidence that loops with arbitrarily small values of γ^0 may not exist, we have written a computer code which searches the space of piecewise linear loop trajectories for the loop with the minimum value of γ^0. The results of this search are preliminary; however, after examining tens of thousands of loops, the minimization routine has yet to find a loop with γ^0 less than the above value of $\gamma^0 \cong 39.003$. Taken together, this evidence leads us to make the following conjecture.

Conjecture. In the center-of-mass frame, there exists a minimum gravitational radiation rate $\gamma^0_{\rm min} > 0$ *for all cosmic string loops.*

While the value of $\gamma^0_{\rm min}$ is not known, there is evidence that it may equal 39.003... . Figure 8(a) shows the **a** and **b** loops for the string loop with the smallest known value of γ^0, as described above. This loop is *known* to have the minimum value of γ^0 for any loop in the special class of loops for which the **a** loop lies along a line and the **b** loop lies in the plane orthogonal to that line. Figures 8(b)–8(d) show the **a** and **b** loops for the three string loops generated by our fragmentation code which have the lowest values of γ^0. All the string loops have been boosted into their center-of-mass frames and all are seen to have very similar **a** and **b** loops. In each case either the **a** or the **b** loop lies approximately along a line, and the other loop lies approximately in the plane orthogonal

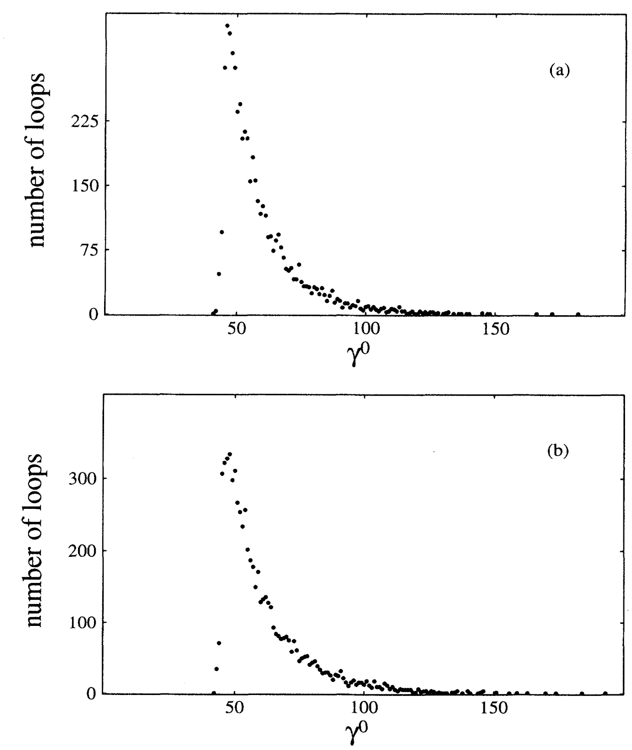

FIG. 7. The number of stable child loops with a given rate of energy loss in gravitational radiation, in units of $G\mu^2$, for loops having initial parent loops of (a) type A and (b) type B. The bins have unit width.

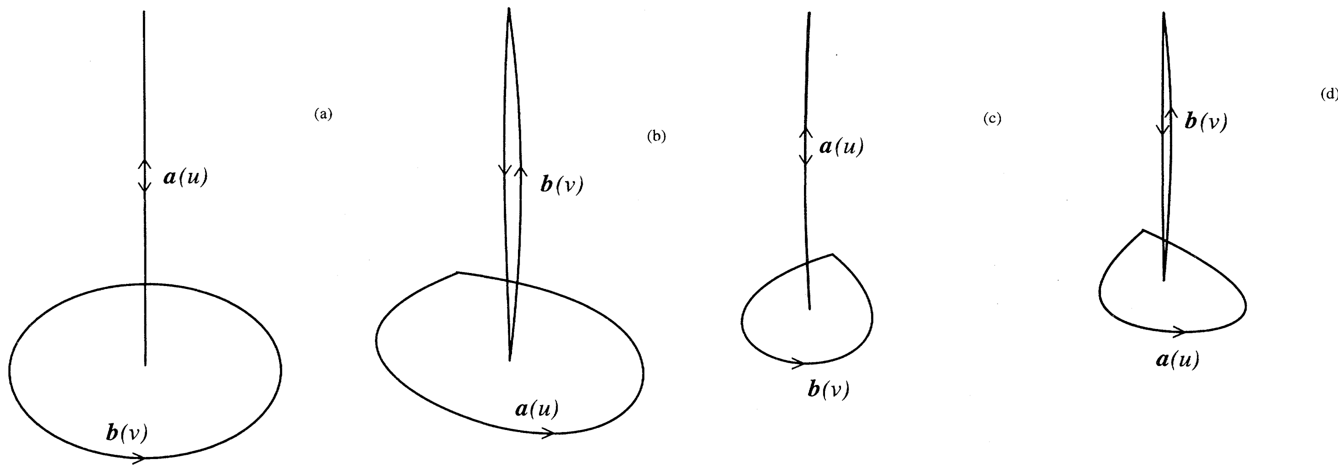

FIG. 8. The **a** and **b** loops defining (a) the string loop with the lowest known value of γ^0 and (b)–(d) the three string loops generated by our fragmentation code with the lowest values of γ^0. The radiation rates for loops (a)–(d) are $\gamma^0 \cong (39.003, 40.898, 41.506, 41.620)$, respectively.

to that line. The loop that lies in the plane has a near circular shape, although in each case the fragmentation process has left one kink on the loop. Out of 11 625 loops examined, only six had $\gamma^0 < 42$. All six of these loops have the same general shape as the loop with the smallest known value of γ^0. Based on this evidence we make the following conjecture.

Conjecture. The value of $\gamma^0_{\rm min}$ *is* $\gamma^0_{\rm min} = 39.003...$ *and is obtained from a cosmic string loop defined by an* **a** *loop that has two straight segments along a line and a circular* **b** *loop (traversed once) in the plane orthogonal to that line.*

Note that this second conjecture implies the first. While we do not have a formal proof of either conjecture, there is additional compelling evidence which supports them.

Additional evidence for our conjectures was found by investigating the correlation between the rate at which cosmic string loops radiate gravitational waves and the velocity of the loops as they oscillate in their center-of-mass frame. One may easily prove that in the center-of-mass frame the square of the velocity averaged over one period of oscillation has a constant value for any cosmic string loop:

$$\frac{\int_0^L d\sigma \int_0^{L/2} dt\, \dot{\mathbf{x}}^2(\sigma,t)}{\int_0^L d\sigma \int_0^{L/2} dt} = \frac{1}{L^2}\int_0^L du \int_0^L dv\, \dot{\mathbf{x}}^2(u,v) = \frac{1}{2}, \tag{3.7}$$

where $u \equiv t+\sigma$ and $v \equiv t-\sigma$. However, this does not mean that each point on the loop moves with velocity $1/\sqrt{2}$ at each moment in time. In order to measure the deviation of the square of the loop's velocity from 1/2, we compute the variance

$$s^2 = \frac{\int_0^L du \int_0^L dv\, \left[\dot{\mathbf{x}}^2(u,v) - \frac{1}{2}\right]^2}{\int_0^L du \int_0^L dv} = \frac{1}{4L^2}\int_0^L du \int_0^L dv\, \left[\mathbf{a}'(u)\cdot\mathbf{b}'(v)\right]^2, \tag{3.8}$$

where a prime means differentiation with respect to the function's argument. It is clear from this equation that s^2 is nonnegative and lies in the range $s^2 \in [0, 1/4]$. We have computed s^2 for each for the 11 625 non-self-intersecting child loops for which γ^α has been calculated. Figure 9 shows a scatter plot of γ^0 vs s^2 for each of the child loops. Here, we have included loops descended from both type A and type B parent loops on the same plot. The individual scatter plots are virtually indistinguishable.

The most important feature of Fig. 9 is that there appears to be a lower bound on γ^0 for each value of s^2, and the curve defining this lower boundary appears to be a monotonically increasing function of s^2. This suggests very strongly that, in the center-of-mass frame, if there is a cosmic string loop with an absolute minimum value of γ^0, then it will be a loop which has $s^2 = 0$. However, one can easily prove that the *only* string loops which have $s^2 = 0$ are exactly the loops where either the **a** or **b** loop lies along a line, and the other loop lies in the plane perpendicular to that line. (Here we shall assume, without loss of generality, that it is the **a** loop which lies along a line.) When a **a** loop is composed of two equal length, co-linear straight segments, then the string loops belong to the special class of loops investigated in [10]. When the **a** loop is composed of an even number (more than two) of co-linear straight segments, then the string loops no longer belong to this special class of loops. However, in this case numerical investigations have shown that, as one would expect, the additional complexity in the string loop trajectories caused by the additional segments on the **a** loop (for any fixed **b** loop) inevitably leads to a larger vlaue of γ^0. Thus the string loop identified in the

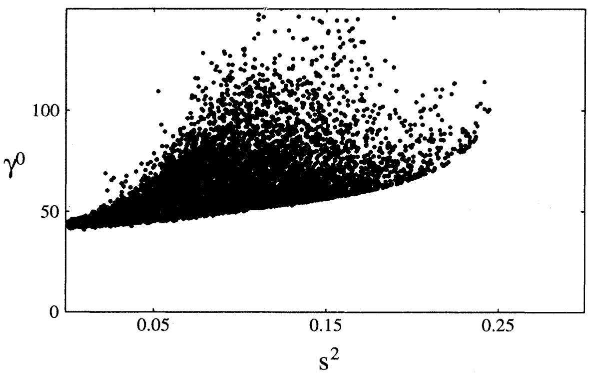

FIG. 9. Scatter plot of γ^0 vs s^2 for 11 625 child loops descended from both type A and type B parent loops. s^2 is the variance of the loop's squared velocity [Eq. (3.8)]. This figure suggests that there is a lower boundary corresponding to a minimum value of γ^0 for any value of s^2. It also suggests that the curve defining this lower boundary increases monotonically as a function of s^2.

second conjecture is the loop which appears to have the absolute lowest value of γ^0 among the class of loops with $s^2 = 0$. While the numerical evidence provided by Fig. 9 does not prove either of our conjectures, it does give them considerable additional support.

If a loop radiates its energy asymmetrically, then the loop will also radiate spatial momentum. When a loop radiates momentum in a given direction, it begins to recoil and accelerate in the opposite direction. This is known as the rocket effect. The magnitude of the total radiated spatial momentum of a loop is given in the center-of-mass frame by

$$\left|\frac{\Delta \mathbf{P}}{\Delta \tau}\right| = \left[\left(\frac{\Delta P_x}{\Delta \tau}\right)^2 + \left(\frac{\Delta P_y}{\Delta \tau}\right)^2 + \left(\frac{\Delta P_z}{\Delta \tau}\right)^2\right]^{\frac{1}{2}} . \quad (3.9)$$

The number of child loops with a given total radiated momentum is shown in Fig. 10. Figures 10(a) and 10(b) show the results for loops descended from type A and type B parents, respectively. The shapes of the two distributions are very similar. In both cases, the majority of loops radiate only a small amount of momentum. If M and τ are the mass and lifetime of a child loop, respectively, then the velocity the loop gains due to the rocket effect is approximately $v_r \sim (\dot{P}/M)\tau \sim (\dot{P}/\dot{E}) \lesssim 0.1$. This is small compared to the typical velocity a child loop acquires at its formation (see Fig. 5).

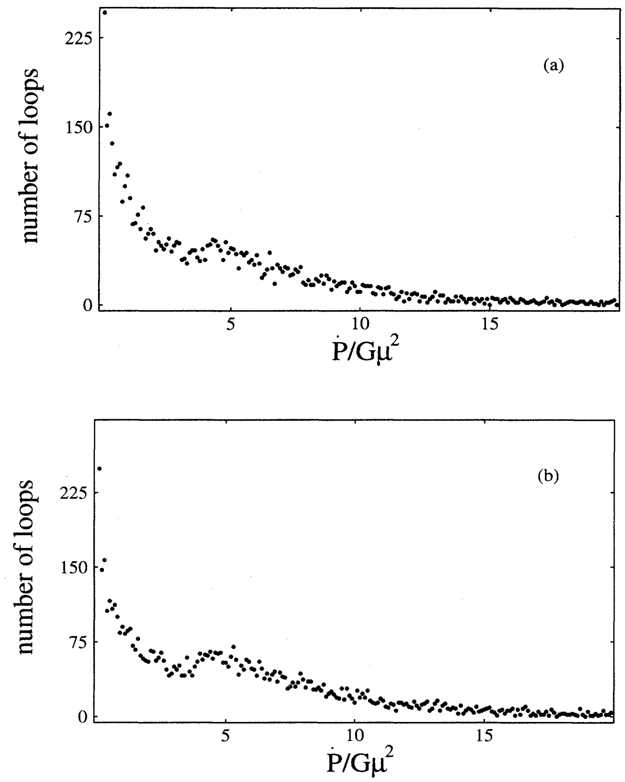

FIG. 10. The number of stable child loops with a given rate of spatial momentum loss in the center-of-mass frame, in units of $G\mu^2$, for loops having initial parent loops of (a) type A and (b) type B. Each bin has a width of 1/10.

IV. CONCLUSION

We have generated and examined a large number of realistic cosmic string loop trajectories. The trajectories were found by using a numerical fragmentation procedure similar to that of Scherrer and Press [11]. Our fragmentation code has been successfully tested on a large set of loops for which the self-intersection points are known analytically. Initial parent loops from two very different classes were evolved forward in time until they self-intersected. Once a loop self-intersects, it fragments into two child loops. The child loops are then fragmented recursively until only non-self-intersecting loops remain. The set of stable child loops has been examined and compared with the loops generated by Scherrer and Press. We find that the loops generated by the two different fragmentation codes are similar, though the improved statistics and higher resolution of our code have identified a some what larger number of small, high velocity loops.

The rates at which the stable child loops radiate energy and momentum have been calculated in several different reference frames. In the center-of-mass frame the radiated spatial momentum is typically small. Thus the distribution of energy radiation rates appears similar in any frame and the velocity gained due to the rocket effect is negligible compared to the velocity a loop is formed with. The distribution of gravitational radiation rates is found to be highly peaked in the range $\gamma^0 = 45$–55 and falls off rapidly for larger values of γ^0. There is a sharp cutoff in the distribution for lower values of γ^0, with absolutely none of the loops having $\gamma^0 < 40$. This, along with substantial other evidence, leads us to conjecture that in the center-of-mass frame there is a minimum value $\gamma^0_{\rm min} > 0$

of the string radiation. Because the **a** and **b** loops for all of the child loops with $\gamma^0 < 42$ have roughly the same shape as the **a** and **b** loops describing the loop with the lowest known value of γ^0, and because in the center-of-mass frame this loop appears to have the minimum value of γ^0 within the class of string loops with $s^2 = 0$, we conjecture that this loop has the smallest radiation rate in the center-of-mass frame for *all* cosmic string loops, and that $\gamma^0_{\rm min} \cong 39.003$. It is hoped that future work will result in a formal proof of one or both of the conjectures.

Note added in proof. Since the time this paper was submitted, we have generated and investigated a total of 12 830 additional child loops descended from two new sets of initial parent loops. These two new parent loop types differ from the A and B type loops in that the first set of loops are defined to have 20 modes (with amplitudes chosen in the same manner as the type A loops), and the second set have 5 modes (with amplitudes chosen in the same manner as the type B loops). This additional investigation has shown that the distributions of radiation rates (shown in Fig. 7 and 10), and the correlation between the gravitational radiation rate and the variance of the loops squared velocity (shown in Fig. 9) do *not* depend on the number of modes used to define the initial parent loops. This provides additional evidence that the cosmic string loop trajectories investigated in this paper are representative of generic, realistic loop trajectories.

ACKNOWLEDGMENTS

This work was supported in part by NSF Grants No. PHY-91-05935 and PHY-95-07740, and by a grant from the Wisconsin Space Grant Consortium and the National Space Grant College Program. We would like to thank Dr. R. Scherrer and Dr. J. Quashnock for many useful exchanges concerning their work and for providing the data to which we compared our results. We are also grateful to Adrian Ottewill for his collaboration in much of this, and related work.

[1] T. W. B. Kibble, J. Phys. A **9**, 1387 (1976); T. W. B. Kibble, G. Lazarides, and Q. Shafi, Phys. Rev. D **26**, 435 (1982).
[2] Y. B. Zel'dovich, Mon. Not. R. Astron. Soc. **192**, 663 (1980).
[3] A. Vilenkin, Phys. Rev. D **24**, 2082 (1981); Phys. Rep. **121**, 263 (1985).
[4] E. P. S. Shellard and A. Vilenkin, *Cosmic Strings and other Topological Defects* (Cambridge University Press, Cambridge, England, 1994).
[5] R. R. Caldwell and B. Allen, Phys. Rev. D **45**, 3447 (1992).
[6] R. R. Caldwell, in *General Relativity and Relativistic Astrophysics*, Proceedings of the Fifth Canadian Conference, Waterloo, Canada, 1993, edited by R. Mann and R. McLenaghan (World Scientific, New York, 1993).
[7] T. Vachaspati and A. Vilenkin, Phys. Rev. D **31**, 1052 (1985).
[8] C. Burden, Phys. Lett. **164B**, 277 (1985).
[9] D. Garfinkle and T. Vachaspati, Phys. Rev. D **36**, 2229 (1987).
[10] B. Allen, P. Casper, and A. Ottewill, Phys. Rev. D **50**, 3703 (1994).
[11] R. Scherrer and W. Press, Phys. Rev. D **39**, 371 (1989).
[12] R. Scherrer, J. Quashnock, D. Spergel, and W. Press, Phys. Rev. **D 42**, 1908 (1990).
[13] J. M. Quashnock and D. N. Spergel, Phys. Rev. D **42**, 2505 (1990).
[14] B. Allen and P. Casper, Phys. Rev. D **50**, 2496 (1994).
[15] B. Allen, P. Casper, and A. Ottewill, Phys. Rev. D **51**, 1546 (1995).
[16] F. Embacher, Phys. Rev. D **46**, 2381 (1992).
[17] C. J. Hogan, Nature (London) **326**, 853 (1987).
[18] N. Turok, Nucl. Phys. **B242**, 520 (1984).
[19] J. D. Jackson, *Classical Electrodynamics* (Wiley, New York, 1975), Eq. 11.19.
[20] J. M. Quashnock (private communication).